JGR Oceans

RESEARCH ARTICLE
10.1029/2024JC020983

The Variability of the Size Distributions of Submicron Particles in the Oceans

Yuanheng Xiong[1], Xiaodong Zhang[1], Yannick Huot[2], Brandon M. Stephens[3,4], and Craig A. Carlson[3]

[1]Division of Marine Science, School of Ocean Science and Engineering, Stennis Space Center, The University of Southern Mississippi, Ocean Springs, MS, USA, [2]Department of Applied Geomatics, Université de Sherbrooke, Sherbrooke, QC, Canada, [3]Marine Science Institute and Department of Ecology, Evolution and Marine Biology, University of California, Santa Barbara, CA, USA, [4]Institute of Oceanography, National Taiwan University, Taipei, Taiwan

Key Points:

- Bacterioplankton are a dominant component, accounting for 30%–90% of submicron particles
- At the North Pacific surface, submicron particle sizes increased by ∼5% from dawn to noon, likely due to diurnal growth of bacterioplankton
- A storm at the North Atlantic site introduced a different submicron particle population that was ∼10% larger in mean size

Correspondence to:
Y. Xiong,
yuanheng.xiong@usm.edu

Citation:
Xiong, Y., Zhang, X., Huot, Y., Stephens, B. M., & Carlson, C. A. (2024). The variability of the size distributions of submicron particles in the oceans. *Journal of Geophysical Research: Oceans*, *129*, e2024JC020983. https://doi.org/10.1029/2024JC020983

Received 30 JAN 2024
Accepted 26 SEP 2024

Author Contributions:
Conceptualization: Xiaodong Zhang
Data curation: Yuanheng Xiong, Brandon M. Stephens
Formal analysis: Yuanheng Xiong
Funding acquisition: Xiaodong Zhang, Yannick Huot, Craig A. Carlson
Investigation: Yuanheng Xiong, Xiaodong Zhang, Brandon M. Stephens, Craig A. Carlson
Methodology: Yuanheng Xiong, Xiaodong Zhang
Project administration: Xiaodong Zhang
Supervision: Xiaodong Zhang
Validation: Yannick Huot
Visualization: Yuanheng Xiong
Writing – original draft: Yuanheng Xiong
Writing – review & editing: Xiaodong Zhang, Yannick Huot, Brandon M. Stephens, Craig A. Carlson

Abstract The size distribution of submicron particles is essential for understanding their biogeochemical and optical roles, but it has seldom been measured. This study utilizes ViewSizer 3000, an instrument that tracks Brownian motions of particles, to measure the particle size distributions (PSD) from 250 to 1,050 nm in the North Pacific Ocean (NP) and the North Atlantic Ocean (NA) at depths from 5 to 500 m. The concentration of particles varies over one order of magnitude at any given size bin, with greater variations up to two orders of magnitude at sizes >600 nm. In both locations, concentrations decrease with depth. Bacterioplankton are a dominant component, accounting for 65%–90% of the submicron particles in the surface waters (<100 m) and approximately 30%–40% at depths >150 m at both sites. In the NP, the volume mean diameter increased approximately 5% from the morning to noon at the surface, probably resulting from the diurnal growth of bacterioplankton. In the NA, the concentration and mean size increased by >60% and ∼10% respectively after one storm that introduced a different particle population into the study area.

Plain Language Summary This study investigates the abundance of particles of sizes from 250 to 1,050 nm in the North Pacific Ocean (NP) and North Atlantic Ocean (NA). These submicron particles have seldom been measured but play an important role in various biogeochemical processes and light interactions in the ocean. We found that the abundances of submicron particles, while differing at various locations by up to two orders of magnitude, generally decrease with depth. Most of these submicron particles are bacterioplankton, making up 65%–90% of these particles near the surface and about 30%–40% in depths greater than 150 m. We observed a ∼5% increase of mean size in the surface water of NP from morning to noon, probably resulting from the diurnal growth of bacterioplankton. We also observed an increase of 60% in abundance and 10% in size in the NA after one storm that introduced a different particle population into the study area.

1. Introduction

Submicron particles in the global oceans comprise colloids, viruses, bacteria, and picophytoplankton, which together play a critical role in the biogeochemical cycling of nutrients and organic matter (Filella, 2006; Guo & Santschi, 1997; Kepkay, 1994). Submicron particles are small enough to be insensitive to gravitational settling yet abundant enough to contribute significantly to carbon export through adsorption and aggregation (Jackson, 1988; Kepkay, 1994; Koike et al., 1990; Sharp, 1973; Stramski & Wozniak, 2005; Toggweiler, 1990), and downward mixing (Carlson et al., 2010; Omand et al., 2015; Richardson & Jackson, 2007). Submicron particles are believed to be optically important, especially for backscattering (Stramski & Kiefer, 1991; Stramski & Wozniak, 2005; Zhang et al., 2020), even though larger, phytoplankton-type particles were also found to contribute significantly to backscattering in many aquatic environments (Dall'Olmo et al., 2009; Organelli et al., 2020). To better understand the biogeochemical and optical roles of submicron particles, it is essential to have knowledge of both their size and abundance, as described by the particle size distribution (PSD).

Various measurements and techniques have been used to obtain the PSD of submicron particles (Table 1, Figures 1 and 2). Using a transmission electron microscope (TEM), Wells and Goldberg (1991, 1992, 1994) found that particles of sizes <200 nm in the coastal water off California, in the North Atlantic Ocean and the Southern Ocean, have concentrations $>10^9$ ml^{-1} and depth distributions varying significantly across the sampling sites. Many studies have used commercially available resistive pulse particle counters, Elzone Particle Size Analyzer and/or Multisizer Coulter Counter, to measure submicron particles in seawater. In the North Pacific Ocean near

Journal of Geophysical Research: Oceans

10.1029/2024JC020983

Table 1
Measurements of Size Distributions of Submicron Particles in Seawater

Study	Size range [nm]	Concentration (<1,000 nm) [ml^{-1}]	PSD slope (<1,000 nm)	Sampling location	Instrument
Koike et al. (1990)	380–1,000	6×10^5–8×10^7	–	The North Pacific near Japan	Elzone (12 μm aperture)
Wells and Goldberg (1991)	5–120	$2.00 \pm 0.63 \times 10^9$	1.03 ± 0.36[a]	Santa Monica Basin	TEM
Wells and Goldberg (1992)	5–120	$2.77 \pm 0.86 \times 10^9$	1.75 ± 0.22[a]	Near San Diego, CA	TEM
Wells and Goldberg (1994)	5–200	$3.38 \pm 1.43 \times 10^9$	1.45 ± 0.26[a]	The North Atlantic Ocean and Southern Ocean	TEM
Longhurst et al. (1992)	450–1,000	$2.31 \pm 1.67 \times 10^6$	12.19 ± 1.95[a]	The North Atlantic near Nova Scotia	Elzone and Coulter Counter (12 μm and 14 μm aperture)
Yamasaki et al. (1998)	430–1,000	$1.24 \pm 1.00 \times 10^6$	12.04 ± 1.87[a]	The North Pacific near Japan	Elzone (12 μm aperture)
Loisel et al. (2006)	600–17 μm	$2.22 \pm 1.45 \times 10^4$	6.26 ± 1.26	The south tropical Pacific	Coulter Counter (30 μm aperture)
Gallego-Urrea et al. (2010)	~100–500	$8.40 \pm 2.46 \times 10^7$	3.78 ± 1.73	Coastal water near Sweden	NanoSight
Agagliate et al. (2018)	500–10 μm	$1.69 \pm 1.59 \times 10^5$	3.27 ± 0.49	Coastal water near UK	CytoSense Flow Cytometer
Organelli and Dall'Olmo (2018)	600–12 μm	$3.12 \pm 2.77 \times 10^4$	6.07 ± 0.81	The Atlantic Ocean	Coulter Counter (20 μm aperture)
Reynolds and Stramski (2021)	700–18 μm	$2.74 \pm 1.56 \times 10^5$	5.97 ± 2.57	The Arctic	Coulter Counter (30 μm aperture)
Reynolds and Stramski (2021)	700–18 μm	$6.56 \pm 5.26 \times 10^4$	4.94 ± 1.18	The Atlantic Ocean	Coulter Counter (30 μm aperture)
Reynolds and Stramski (2021)	700–18 μm	$3.14 \pm 1.11 \times 10^4$	4.52 ± 1.30	Near Hawaii, HI	Coulter Counter (30 μm aperture)
Reynolds and Stramski (2021)	800–>1,000	$6.88 \pm 4.21 \times 10^4$	5.62 ± 1.97	Santa Barbara Channel, CA	Coulter Counter (30 μm aperture)
Current study	250–1,050	$5.24 \pm 1.98 \times 10^5$	3.32 ± 0.38	The North Pacific Ocean near Station Papa	ViewSizer 3000
Current study	250–1,050	$5.96 \pm 2.47 \times 10^5$	3.23 ± 0.44	The North Atlantic Ocean tracking an eddy	ViewSizer 3000

[a]Based on data extracted from the figures in the publications.

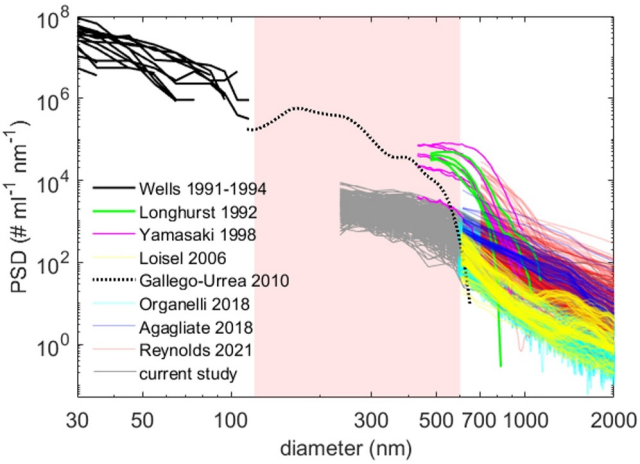

Figure 1. Particle size distributions (PSD) measured in the previous studies listed in Table 1 (colored lines) and in this study (gray lines). The red shaded area indicates the size gap between 120 and 600 nm that few data had been collected.

Japan, Koike et al. (1990) measured particles between 380 and 1,000 nm with concentrations varying from 6×10^5 ml^{-1} to 8×10^7 ml^{-1}. In the same region, Yamasaki et al. (1998) found the submicron particles exhibiting a peak in distribution near 600 nm with total concentrations varying from 5×10^4 ml^{-1} to 3×10^7 ml^{-1}. In both studies, the particle concentrations correlated strongly with the concentrations of chlorophyll-a and microbes, such as bacteria and heterotrophic flagellates. Longhurst et al. (1992) found particles of sizes between 450 and 1,000 nm varying from 6.26×10^6 ml^{-1} to 1.59×10^7 ml^{-1} in the North Atlantic Ocean near Nova Scotia, exhibiting a peak in distribution around 500 nm.

In more recent studies, Loisel et al. (2006) and Organelli and Dal-l'Olmo (2018) measured particle size distributions in the South Tropical Pacific Ocean and along a transect in the Atlantic Ocean, respectively. In both studies, the power-law slopes of PSDs at sizes from 600 to 1,000 nm averaged around six, twice as steep as the slopes estimated for particles greater than 1,000 nm. The steeper slope indicates the relatively higher concentration of smaller particles. Organelli et al. (2020) suggested that the steeper slope values of PSDs, with sizes peaking around 600 nm, are likely related to *Prochlorococcus*. Their PSDs only covered the larger half of the peak, resulting in higher slope values. Reynolds and Stramski (2021) reported

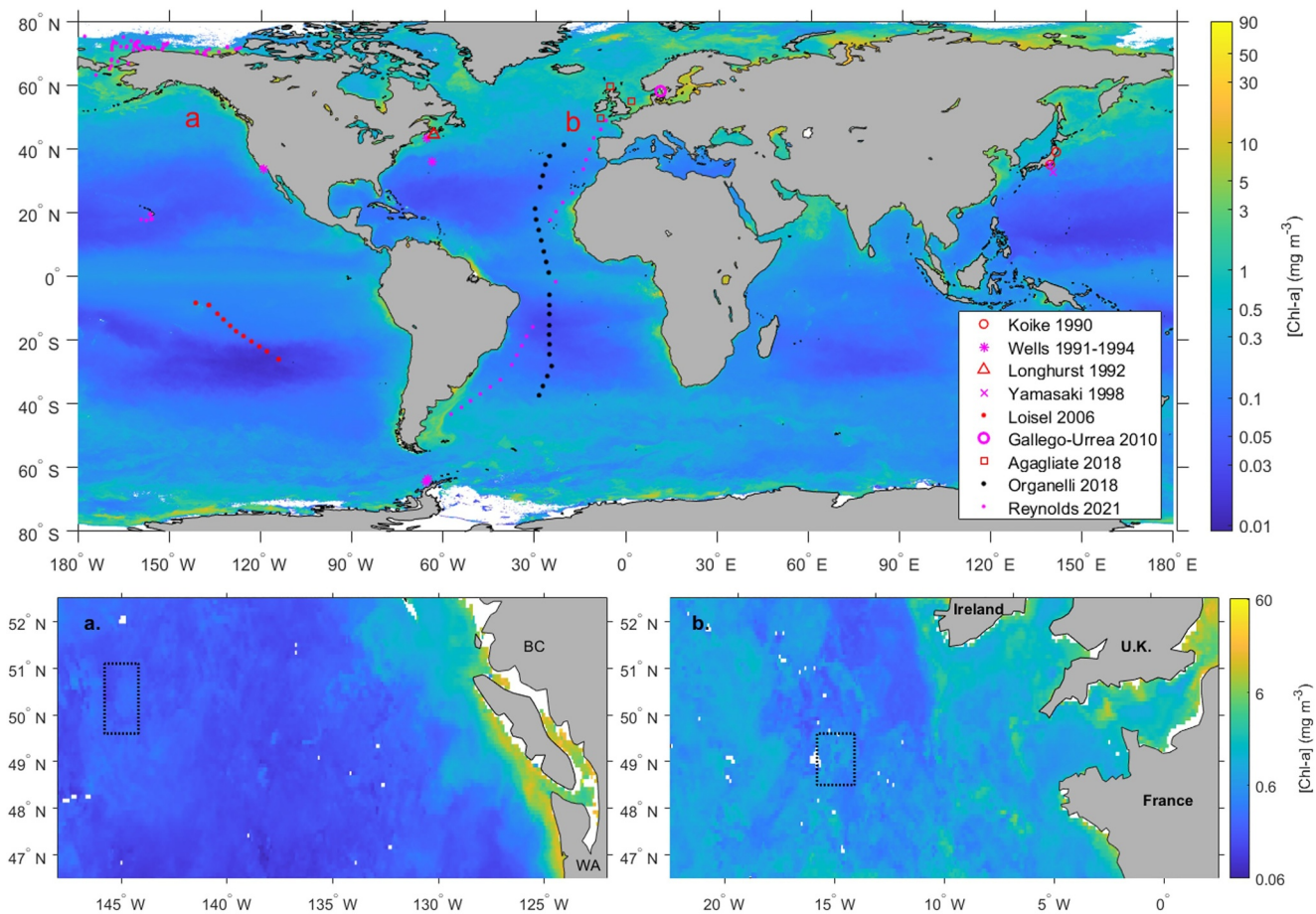

Figure 2. A global view of experiment locations of studies listed in Table 1 overlaid on 2022 annual mean MODIS-derived Chlorophyll-a concentration, and the sampling areas (the dashed rectangles) of current study overlaid on mean MODIS-derived Chlorophyll-a concentration for (a) July–September 2018 in the North Pacific Ocean (NP) and (b) May 2021 in the North Atlantic Ocean (NA).

measurements of particles >700 nm in various locations worldwide and the average slope values vary from 4.52 to 5.97. Using a flow cytometer, Agagliate et al. (2018) measured particles >500 nm in the UK shelf waters and reported a mean slope value of 3.27 ± 0.49.

To test NanoSight, an instrument that tracks the Brownian motion of particles to estimate their sizes (Einstein, 1905; Langevin, 1908), Gallego-Urrea et al. (2010) measured a water sample collected in coastal waters of Sweden and estimated a total concentration of 8.4×10^7 ml^{-1} for particles of sizes between 50 and ∼500 nm. They also noted that the concentration was underestimated for particles smaller than ∼100 nm. Among these limited efforts in resolving submicron particles, there were few PSDs measured between 120 and 600 nm (highlighted as a red shaded area in Figure 1). Even for PSDs between 600 and 1,000 nm, there were significant differences in the slope values. Those measured by Longhurst et al. (1992) and Yamasaki et al. (1998) exhibit slope values averaging around 12, much steeper than the others (Figure 1).

We used a ViewSizer 3000 (Stramski et al., 2017) to measure the size distribution of submicron particles. The ViewSizer 3000 uses three laser beams to track Brownian motion, improving over the single wavelength laser beam deployed in NanoSight to better resolve natural particles that are polydispersed (Stramski et al., 2017). Xiong et al. (2022) conducted a Monte Carlo simulation and lab calibrations using microbeads of NIST-traceable sizes to evaluate the performance of the instrument. They found that the ViewSizer 3000 can resolve particles of sizes between 250 and 1,050 nm with a mean absolute error of 3.9% in size and 38% in concentration. We deployed the ViewSizer 3000 for the first time in the field during the NASA Export Processes in the Ocean from Remote Sensing (EXPORTS) campaigns in the North Pacific and North Atlantic oceans. The measured PSDs (Figure 1 gray lines) help to fill the size gap where limited data had been collected. The primary objective of this study was to examine the variability of submicron particles in the North Pacific and North Atlantic Oceans.

2. Data Collection

2.1. Seawater Sample Collection

We participated in the EXPORTS field campaign (Siegel et al., 2021) in the North Pacific (NP) near the Ocean Station Papa (50°N, 145°W) (Leipper, 1954) aboard R/V *Sally Ride* in August/September 2018, and in the North Atlantic (NA) tracking an eddy core (49°N, 15°W) aboard the RRS *Discovery* in May 2021 (Figure 2). The mean seasonal Chlorophyll-a concentration over the study areas, as derived from MODIS, is 0.22 ± 0.04 mg m^{-3} for the NP and 0.58 ± 0.19 mg m^{-3} for the NA.

The experiment in the NP lasted 28 days. Water samples were collected at depths between 5 and 500 m by Niskin bottles attached to a conductivity-temperature-depth (CTD) rosette. Two CTD casts were performed daily, one in the morning between 06:00 and 10:00 and the other around noon between 11:00 and 15:00. Seven nominal depths (5, 15, 25, 50, 75, 150, and 330/500 m) were preset, with 330 m used for the morning cast and 500 m for the noon cast. The final collection depths were adjusted according to the measured CTD data. The water sample collected at each depth was drained into a 10 L carboy, which was then either measured immediately or stored in a 4°C walk-in fridge for later measurement. All PSD measurements were conducted within 5 hr of collection, and the depths of the samples to be measured were chosen randomly. Before each measurement, seawater was pipetted from the 10 L carboy into a 20 ml borosilicate glass for transport to the instrument.

In the NA, the cruise spent 25 days tracking an eddy located inside the dashed rectangle area in Figure 2b. The sampling stations for our PSD measurements were all within the eddy core (L. Johnson et al., 2023). The experiment was separated into three Epochs, mainly demarcated by three major storm events. Only one cast of samples was collected daily between 1,200 and 1,500 at eight nominal depths (5, 20, 35, 50, 75, 110, 150, and 500 m) and adjusted as described above.

2.2. Operating the ViewSizer 3000

The ViewSizer 3000 used at sea was set up and operated according to Xiong et al. (2022). Briefly, a 3 mL quartz cuvette containing the water sample was placed in the observation chamber of the ViewSizer 3000. The chamber was illuminated by laser beams at three wavelengths, 450, 520, and 650 nm, and light scattered by each particle at 90° relative to the incident beam was recorded. Because the scattering by submicron particles is proportional to the 4th–6th power of their sizes, the actual sampling volume also increases with the size of particles (Xiong et al., 2022), varying from approximately 2 to 7 nL for sizes from 200 to 1,000 nm. We took 100 of 10-s videos at a

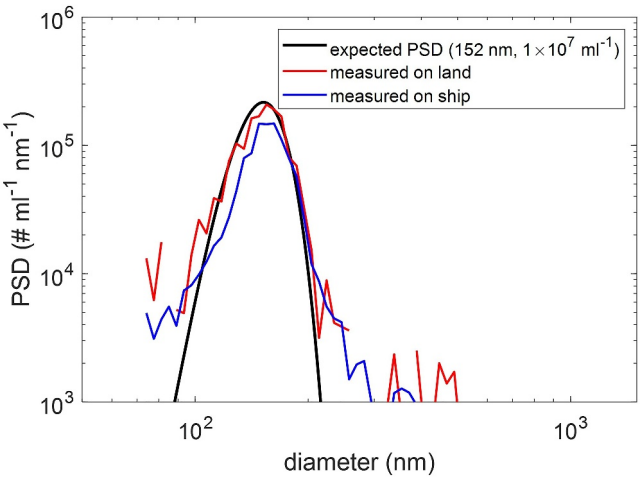

Figure 3. Particle Size Distributions (PSDs) of NIST-traceable standard size microbeads measured by ViewSizer 3000 on land (red) and on the ship (blue) where the instrument was placed on a vibration isolation platform are compared with the expected PSD assuming a normal distribution (black) with a mean diameter of 152 nm, a standard deviation of 19.45 nm, and a concentration of 1×10^7 ml^{-1}.

frame rate of 30 Hz for each sample. The sample was stirred by a magnetic stir bar between videos to ensure adequate mixing of samples. Each 10-s video was analyzed individually to estimate the size of each particle recorded in the video. The estimated sizes are equivalent to the diameter of spherical particles that would go through the same Brownian motion. The estimated sizes were then binned into 12 size ranges centered at 234.42, 269.15, 309.03, 354.81, 407.38, 467.74, 537.03, 616.60, 707.95, 812.83, 933.25, and 1,071.55 nm, with bin width increasing logarithmically from 30.25 to 138.27 nm. The final PSD for the sample was the sum of 100 individual results from each 10-s video. Since each sample took approximately 35 min to finish, we could only measure samples collected at six depths, which always included the top and bottom depths and at least one depth near chlorophyll maximum, if present.

The ViewSizer 3000 was placed on a Newport© VIBe™ VIP320X mechanical vibration isolation platform to dampen the ambient vibration of the ship. We tested the effectiveness of this platform using polystyrene latex beads of NIST-traceable sizes. Figure 3 shows the test result of using beads of nominal size 152 nm with a standard deviation of 19.45 nm, prepared at a concentration of 1×10^7 ml^{-1}. The mode size values and concentrations of the beads measured on land and on ship were 152 nm and 1.03×10^7 ml^{-1}, and 157 nm and 8.29×10^6 ml^{-1}, respectively. The differences in the mode values and concentrations are 3.3% and 18%, which are within the corresponding uncertainties of ViewSizer 3000 that we have calibrated, which are 3.9% and 38%, respectively (Xiong et al., 2022). This suggests that the vibration-isolation platform is effective in damping ambient vibrations. We observed that the vibration-isolation platform is not effective when pitch, roll or heave angles of ship exceed 2°, so we discarded data taken during these higher sea states, which amounted to 10 (~4%) and 23 (~18%) measurements in NP and NA, respectively.

The ViewSizer 3000 tracks the Brownian motion by detecting the light scattered by particles with a camera. The presence of larger particles (>~600 nm) creates a background scattering that could overwhelm the light scattered by smaller particles (<~200 nm), leaving these small particles undetectable and hence leading to their concentration underestimated. As a result, we found a detection limit of ~250 nm for our ViewSizer 3000 based on polydispersed samples, even though the instrument can resolve monodispersed beads of sizes 100 nm or 152 nm very well in the lab (Xiong et al., 2022) (also see Figure 3). However, this lower limit of ~250 nm was determined in the lab using a mixture of beads of various sizes. To test if this limit also applies to natural waters, we conducted additional experiments by passing 22 samples through 1.2 μm Whatman™ Puradisc FP 30 syringe filters and compared the PSDs of unfiltered and filtered samples. The mean percentage difference between the two groups of PSDs is approximately 9%, which is less than the 38% uncertainty of ViewSizer 3000 that we have calibrated in Xiong et al. (2022). An example of the comparison for one NA sample is shown in Figure 4. The same tests were also conducted for the NP experiment with the same conclusion that the detection limit of 250 nm we determined in the lab also applies to natural waters. Thus, the results present hereinafter are all based on unfiltered samples.

2.3. Data Processing

For each PSD (N; # ml^{-1} nm^{-1}) we calculated the total particle number concentration and volume mean diameter. The total particle number concentration (C_N; # ml^{-1}) is calculated as:

$$C_N = \int_{d_{\min}}^{d_{\max}} N(d)\,\mathrm{d}d, \tag{1}$$

where d (nm) is the equivalent spherical diameter of particles; $d_{\min}$ and $d_{\max}$ (nm) are the minimum and maximum diameters of the PSD. The $d_{\min}$ and $d_{\max}$ are set as 250 and 1,050 nm for ViewSizer 3000 measurements. The volume mean diameter (d_v; nm) is calculated as:

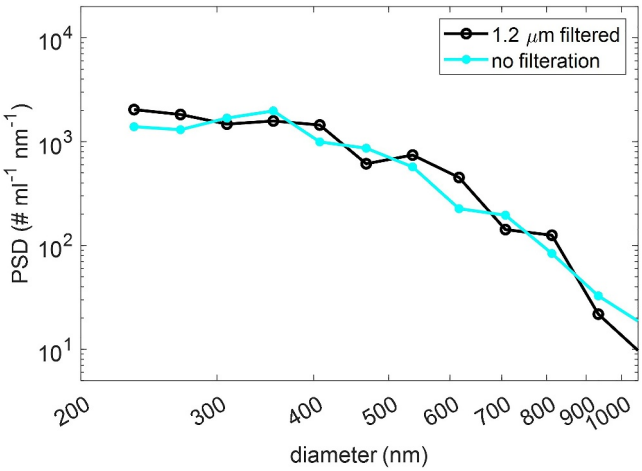

Figure 4. One example of PSDs measured with or without 1.2 μm filtration in the NA.

$$d_V = \left(\frac{\int_{d_{\min}}^{d_{\max}} d^3 N(d) \mathrm{d}d}{C_N} \right)^{1/3}. \quad (2)$$

Meanwhile, the slope (α) is estimated by fitting the PSD to a power-law distribution (Junge, 1969):

$$N(d) = N(d_0)\,(d/d_0)^{-\alpha}, \quad (3)$$

where d_0 is an arbitrary reference diameter set as 1 μm.

3. Results and Discussion

3.1. General Feature

A total of 238 PSDs were measured in the NP and 123 in the NA (Figure 5). The concentration at any given diameter size bin varied by >1 order of magnitude with greater variations up to two orders of magnitude at sizes >600 nm in the NA. The concentration of particles decreased with increasing size. On average, concentrations of submicron particles at 250 nm were approximately 50-fold greater than particles at 1,050 nm.

For each PSD, we calculated the total particle concentration (C_N) and the volume mean diameter (d_v) according to Equations 1 and 2, which are used as a measure of the magnitude and general shape of the PSDs, respectively (Figure 6). C_N varied from approximately 1.5×10^5 to 1.3×10^6 ml^{-1} in both sites, with a mean concentration of 5.96×10^5 ml^{-1} in the NA, approximately 14% greater than the mean 5.24×10^5 in the NP (Figure 6a). d_v varied from 350 to 600 nm across both sites, with the average size in the NA being ~11 nm greater than that in the NP (Figure 6b).

The power-law distribution has been commonly applied to describe the size distribution of oceanic particles, ranging from submicron particles to larger particles such as phytoplankton, zooplanktons and even mammals (Buonassissi & Dierssen, 2010; Corral & González, 2019; Junge, 1969; Sheldon et al., 1972; Wells & Goldberg, 1994). The PSDs in Figure 5 exhibit a change of slope values at sizes around 450 nm, especially for the PSDs measured in the NA. We compared the slopes estimated with Equation 3 over two size ranges, from 250 to 1,050 nm and from 450 to 1,050 nm (Figure 6c). On average, the slope values estimated for particles of size >450 nm are steeper than the values estimated over the entire size range in both the NP and NA, highlighting that the shape of PSDs varies between the two size ranges. This is consistent with recent studies (Loisel et al., 2006; Reynolds & Stramski, 2021; Runyan et al., 2020) that found a single power law relationship is not an appropriate indicator throughout the entire size range. This change of slope might be related to the peak in bacterioplankton

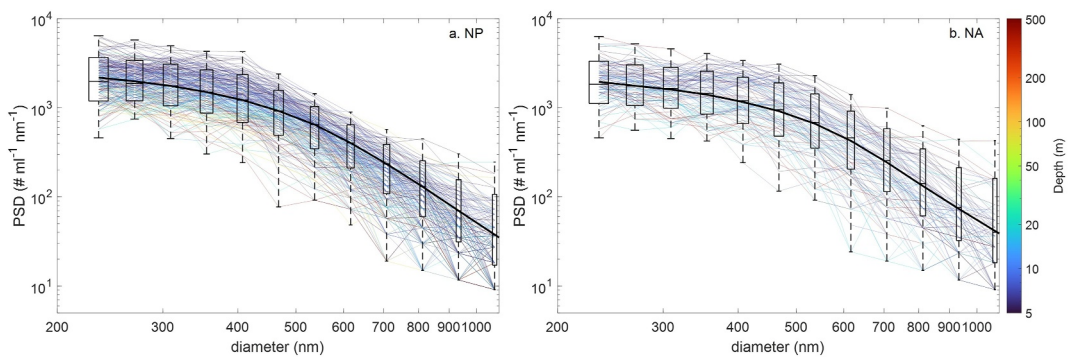

Figure 5. All PSDs measured during the EXPORTS cruise in the NP (a) and during the EXPORTS cruise in the NA (b). Individual measurements are color coded by depth. The black curves are the median value of the PSDs. The whiskers and boxes show the minimum, lower quartile, median, upper quartile, and maximum values.

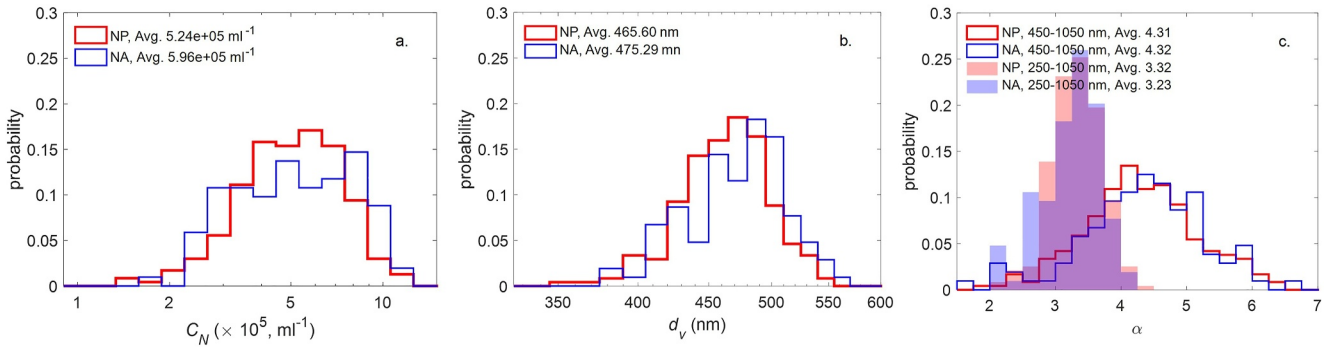

Figure 6. Particle size distributions (PSDs) measured in the NP and NA. (a) total concentrations (C_N), (b) volume mean diameters (d_v), and (c) PSD slopes (α) of the size between 250 and 1,050 nm in the NP (red line) and NA (blue line) and between 450 and 1,050 nm in the NP (filled red) and NA (filled blue).

distribution, which will be discussed later. However, we currently do not have independent data to elucidate the cause of this change in slope for our measurements.

3.2. Vertical Distribution: The North Pacific Ocean

Here we examine the vertical distribution of PSDs grouped by the CTD casts deployed in the morning and around noon time, between which the temperature and salinity only changed slightly (Figures 7a and 7b). The mean C_N values are similar between morning and noon casts, both decreasing with depth from approximately 7.0×10^5 ml^{-1} at the surface to 3.4×10^5 ml^{-1} at 500 m (Figure 7c). The mean d_v value at the surface is 23 nm greater ($p = 0.07$) in noon than in morning casts (Figure 7d), however, no significant difference was observed at deeper depths. This diurnal difference in d_v at the surface might be related to the living components of submicron particles, which will be discussed in Section 3.5.

3.3. Vertical Distribution: The North Atlantic Ocean

The NA experiment was separated into three epochs interrupted by major storms, Epoch 1: 4th to 10th; Epoch 2: 11th to 20th; Epoch 3: 21st to 29th in May 2021 (Figure 8). Epoch 3 introduced warmer (Figure 8a) and saltier (Figure 8b) water into the surface eddy core, deepening the mix layer from ~50 to 100 m. L. Johnson et al. (2023) reported that up to 75% of the water in the upper 100 m had been exchanged between the interior and exterior of the surface eddy core during each storm, and the largest increase in nutrients due to vertical entrainment was

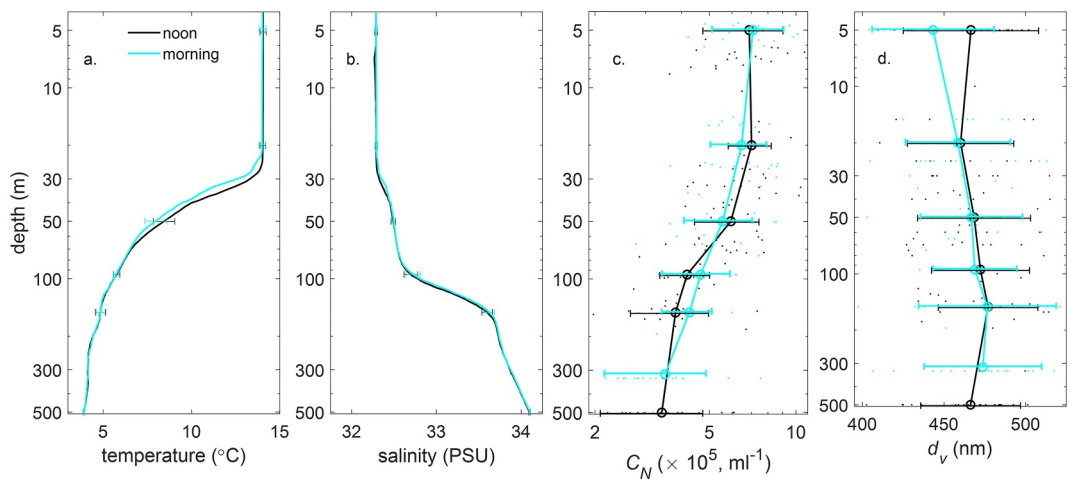

Figure 7. The vertical profiles of (a) temperature, (b) salinity, (c) total concentrations of submicron particles (C_N), and (d) their volume mean diameters (d_v) in the NP. The measurements are grouped by the sampling time: in the morning (black) and around noon (cyan). In (c) and (d), dots are individual measurements, circles the mean values, and horizontal error bars one standard deviation at each depth layer where water samples were collected.

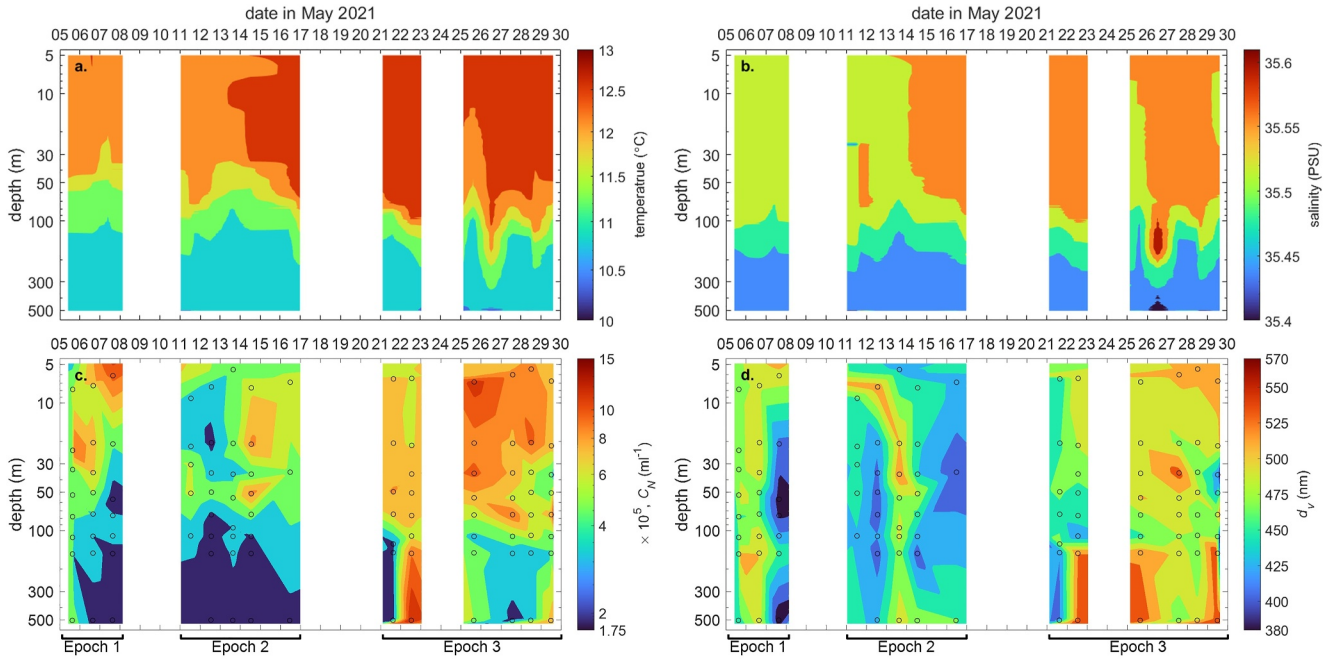

Figure 8. Temporal variation of (a) temperature, (b) salinity, (c) total concentrations of submicron particles (C_N), and (d) their volume mean diameters (d_v) in the NA. The measurements were interrupted by three storms (no data) and separated into three epochs. The black circles in (c) and (d) are individual measurements.

observed between Epoch 2 and 3. Both C_N (Figure 8c) and d_v (Figure 8d) in the upper 100 m decreased slightly from Epochs 1 to 2 by 16.1% and 4.7% respectively, but increased dramatically from Epoch 2 to 3, resulting in approximately a 62.8% increase in C_N and a 20–80 nm increase in d_v between Epochs 2 and 3, probably related to the water mass exchange between the interior and exterior of the surface eddy core during the storms. At depths >100 m, the submicron particle population showed minimal change between Epochs 1 and 2 but increased during Epoch 3 by 68.6% in C_N and 10.1% in d_v, probably due to the deepening of mixed layer between Epochs 2 and 3, bringing surface water mass into the deeper water. Overall, submicron particles exhibit the lowest concentration and smallest size in Epoch 2 whereas the highest concentration and greatest size in Epoch 3.

Clevenger et al. (2024) reported that the particulate organic carbon (POC) to ^{234}Th ratios decreased with depth more rapidly and to a greater extent from Epoch 1 to 3, suggesting that a larger fraction of primary production was being exported to deeper waters during Epoch 3. They also found the biogenic silica (bSi) to ^{234}Th ratios decreased with depth more slowly from Epoch 1 to 3 and remained relatively constant in Epoch 3, supporting that the nature of particle export has been changed in Epoch 3. Our results seem to indicate that the population of submicron particles also changed in Epoch 3 in terms of both concentration and size.

3.4. Global Comparison

As shown in Table 1 and Figure 1, the PSDs between ~600 and 1,000 nm measured in earlier studies (Longhurst et al., 1992; Yamasaki et al., 1998) showed steeper slopes (averaging ~12) than those (averaging ~3–6) measured in more recent studies (Agagliate et al., 2018; Loisel et al., 2006; Organelli & Dall'Olmo, 2018). The resistive pulse particle counters have been used to measure PSDs in nearly all these studies. Longhurst et al. (1992) and Yamasaki et al. (1998) noticed a peak in their PSDs near the measurement limit at smaller sizes, around 500–600 nm, which led to the steep slope values. While we expect that the slopes may vary for different waters, the differences in the slope values may also be due to the inherent difficulties of using a Coulter Counter to measure submicron particles. The size range of particles that a Coulter Counter can detect is determined by the aperture size of the intake, with the lower limit being approximately 2% of the aperture size. The aperture size should be 20 or 30 μm to detect submicron particles. As particles stream through the aperture, the shear force near the aperture entrance may break up larger particles and cause the overestimation of smaller particles as well as the slope values (McCave, 1984). Some recent studies (Reynolds & Stramski, 2021; Runyan et al., 2020) using Coulter Counters

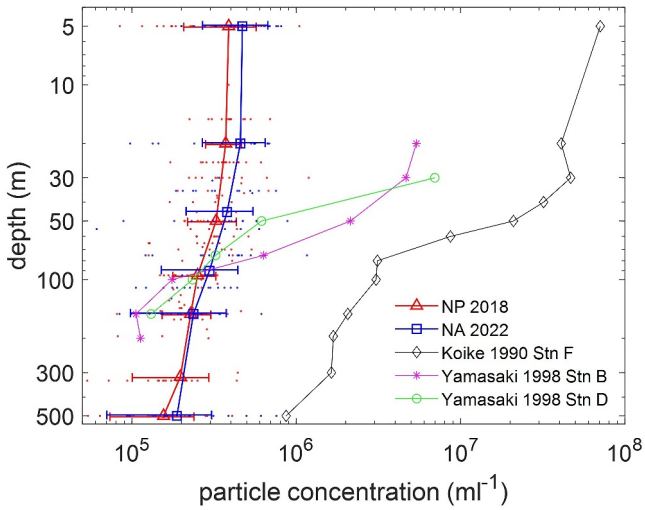

Figure 9. The vertical distribution of submicron particles of sizes from 380 to 1,000 nm measured in the NP and NA (red and blue) and those measured by Koike et al. (1990) (black) and Yamasaki et al. (1998) (magenta and green) in coastal waters of Japan. For NP and NA data, dots represent the data points of individual measurements and horizontal bars their one standard deviation estimated within each depth layer.

were able to measure PSDs of submicron particles down to 600 nm with slopes that are consistent with the results of this study using the ViewSizer 3000, which have a mean slope around 3 and 4.

Koike et al. (1990) and Yamasaki et al. (1998) measured vertical distributions of submicron particles of sizes from 380 to 1,000 nm in the coastal Pacific waters off Japan, and we calculated the concentration over the same size range using our data (Figure 9). In general, submicron particles in the coastal water off Japan showed significantly greater values in near-surface waters, approximately two orders of magnitude greater than the deeper water. Our measurement also shows a decrease from the surface to the deeper water, but the mean concentrations at the surface are approximately 2–4 times of those at 500 m. The elevated surface concentrations in Koike et al. (1990) and Yamasaki et al. (1998) are likely due to greater particle concentrations found in coastal environments, where the Chlorophyll-a concentrations are mostly greater than 1 mg m^{-3} at the surface. In contrast, the open ocean sites in this study have Chlorophyll-a concentrations averaging around 0.22 and 0.86 mg m^{-3} at the surface in the NP and NA, respectively.

3.5. Bacterioplankton

Bacteria are a major living component of the submicron particles (Ducklow & Carlson, 1992; P. W. Johnson & Sieburth, 1979; Koike et al., 1990). The size distributions of bacterioplankton were measured at noon in the same study area during the EXPORTS cruises in the NP and NA but on different ships (RV *Roger Revelle* in NP and RRS *James Cook* in NA). The generation of free living bacterioplankton abundance and size data are described in Stephens et al. (2020). Briefly, bacterioplankton cells were stained with 5 μg mL^{-1} 4′, 6-diamidino-2-phenylindole dihydrochloride (DAPI) and retained on 0.2 μm filters (25 mm polycarbonate). Then, 12 images were captured per sample using a Revolve imaging epifluorescence microscope (Discover Echo, San Diego, CA, USA). Sizes were calibrated using fluorescent beads of known sizes (0.1–1.0 μm), and cell abundances were determined using automated detection methods implemented in imageJ software. Except for a few outliers, which might be due to uncertainties caused by operating on two different ships, the bacterioplankton concentration is generally lower than that of submicron particles in the same size bin (Figures 10a and 10b), which is expected. The bacterioplankton appears to be a dominant component of the submicron particles from 450 to 650 nm in the NP (~91%) and from 250 to 450 nm in the NA (~79%).

As previously mentioned, the change of slope in the PSDs at sizes around 350–450 nm appears as a "flattening" (Figure 5). Similar features were also reported in earlier studies, such as Longhurst et al. (1992) around 500 nm. A closer examination of Figure 5 shows that the "flattening" does not occur in many samples collected from deeper waters and is mainly associated with the samples from near surface waters, where bacterioplankton dominated the

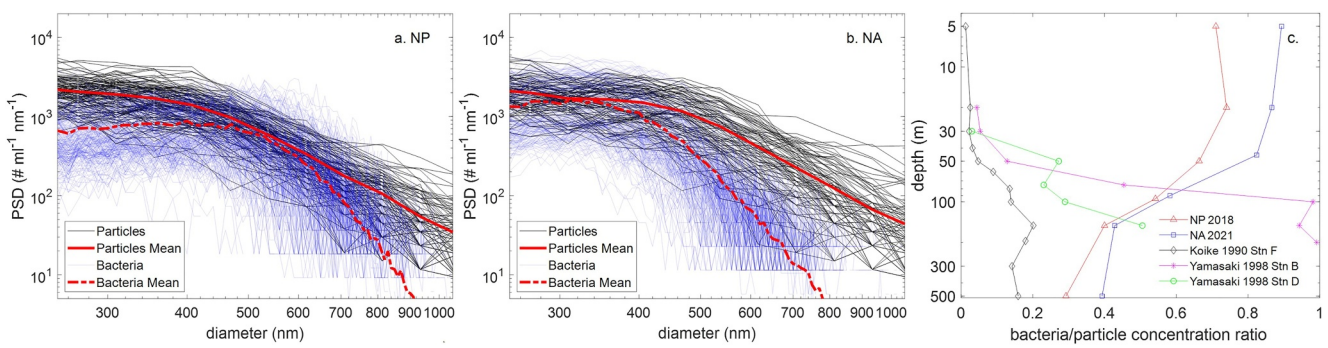

Figure 10. (a) The PSDs of submicron particles (black lines) and bacterioplankton (blue lines) measured in the NP. The red solid and dashed lines are their respective mean values. The noon measurements of the submicron particles are shown. (b) Same as (a) but for measurements in the NA. (c) Depth variations of mean ratios of concentration of bacterioplankton to submicron particles measured in the NP (red) and NA (blue) and those measured by Koike et al. (1990) (black) and Yamasaki et al. (1998) (magenta and green) in the coastal water off Japan.

submicron particles. Furthermore, the "flattening" is more obvious when peaks are observed around 350–450 nm, which roughly align with the peaks of bacterioplankton distribution shown in Figure 10. This suggests that the "flattening" of the overall submicron particle distributions may reflect the peak in bacterioplankton distribution. However, since the bacterioplankton measurements are not paired with our measurements, it is challenging to directly verify this connection.

Across the entire size range of submicron particles, from 250 to 1,050 nm, the average fractional contribution of bacterioplankton in the NP decreases from 74% at 20 m to 30% at 500 m (Figure 10c). The fractional contribution of bacterioplankton in the NA also decreases with depth, from 90% at the surface to 43% at 150 m (Figure 10c). In comparison, the bacterioplankton measured by Koike et al. (1990) and Yamasaki et al. (1998) are less than 10% in the surface coastal water off Japan, indicating that submicron particles in their study area were dominated by non-living particles. Their bacterioplankton contributions increased with depth, reaching approximately 20% at 160 m, and remained relatively constant at deeper depths.

Vaulot and Marie (1999) measured three autotrophic picoplankton groups, *Prochlorococcus*, *Synechococcus*, and *Picoeukaryotes*, in the equatorial Pacific using flow cytometry. They found that the growth in cell size of these picoplankton, particularly *Prochlorococcus* and *Synechococcus*, is initiated at dawn and continues to the early night. For individual cells of the same genera, they observed a ∼15–50% increase in the scattering intensity at 90° from morning to noon, which corresponds to approximately 3%–10% growth in cell size assuming the scattering by these submicron cells proportional to the cell diameter to the power of 4–6. Using SeaFlow data (Ribalet et al., 2020) collected in the North Pacific, Li et al. (2022) reported the size of *Prochlorococcus* and *Synechococcus* increased by ∼11% from 430 to 480 nm, and by ∼7% from 650 to 700 nm, respectively, from morning to noon. We also observed an increase in the mean sizes of submicron particles from 443.28 nm in the morning to 466.49 nm at noon in the NP (Figure 7d), likely due to the diurnal growth of bacterioplankton, which constitute a significant portion of the submicron particles that we have measured (Figure 10). Overall, the comparison of submicron PSD measurements with bacterioplankton concentrations and sizes in the current study has provided an expanded view of how living submicron particles may contribute to all detected submicron particles as a function of depth.

4. Conclusions

We used a Brownian motion tracking instrument, ViewSizer 3000, to measure PSDs in the submicron size range from 250 to 1,050 nm in the NP and NA at depths from 5 to 500 m. The measurements extended the PSD measurements of submicron particles from 600 nm down to 250 nm, filling a size gap that few previous studies could cover (Figure 1 and Table 1). The concentrations of particles vary >1 order of magnitude at any given size bin in both the NP and NA, but generally decrease with depth (Figures 7 and 8). Over the entire water columns that were sampled, the mean concentration in the NA was slightly higher (14%) than in the NP. A single power law relationship could not be applied to the measured PSDs, which showed a change of slope at sizes around 350–450 nm in both sites (Figures 5 and 6). The storm leading to Epoch 3 in the NA introduced a different type of submicron particle population that was approximately 10% larger with greater concentrations. Bacterioplankton appeared to be a dominant component of submicron particles in the surface water (<50 m) of both the NP and NA, accounting for 65%–90% of submicron particles. This dominance decreased with depth, and the fractional concentration was ∼30–40% at depths between 150 and 500 m. The diurnal growth of the bacterioplankton was probably the reason that the volume mean sizes of submicron particles in the surface water of NP increased by ∼5% from dawn to noon (Figure 7d).

Data Availability Statement

The size distributions of submicron particles and bacterioplankton data reported in the study are available at the NASA SeaBASS database (EXPORTS, 2018) via the following links: https://seabass.gsfc.nasa.gov/investigator/Zhang,%20Xiaodong and https://seabass.gsfc.nasa.gov/investigator/Carlson,%20Craig.

Acknowledgments
The authors wish to express their appreciation to the EXPORTS science team for their collaborative contributions, data sharing, and intellectual exchanges. Special thanks are due to the captain and crew of both the R/V *Sally Ride* and RRS *Discovery* for their invaluable work. This project was supported by NASA Grant 80NSSC20K0350 to Xiaodong Zhang and 80NSSC18K0437 to Craig A. Carlson. Brandon M. Stephens was supported in part by the US GO-SHIP postdoctoral fellowship (NSF OCE-2023545). The authors thank Dr. Giorgio Dall'Olmo and an anonymous reviewer for their constructive comments and suggestions that have improved the quality of the manuscript.

References

Agagliate, J., Röttgers, R., Twardowski, M. S., & McKee, D. (2018). Evaluation of a flow cytometry method to determine size and real refractive index distributions in natural marine particle populations. *Applied Optics*, *57*(7), 1705–1716. https://doi.org/10.1364/AO.57.001705

Buonassissi, C. J., & Dierssen, H. M. (2010). A regional comparison of particle size distributions and the power law approximation in oceanic and estuarine surface waters. *Journal of Geophysical Research*, *115*(C10), C10028. https://doi.org/10.1029/2010JC006256

Carlson, C. A., Hansell, D. A., Nelson, N. B., Siegel, D. A., Smethie, W. M., Khatiwala, S., et al. (2010). Dissolved organic carbon export and subsequent remineralization in the mesopelagic and bathypelagic realms of the North Atlantic basin. *Deep Sea Research Part II: Topical Studies in Oceanography*, *57*(16), 1433–1445. https://doi.org/10.1016/j.dsr2.2010.02.013

Clevenger, S. J., Benitez-Nelson, C. R., Roca-Martí, M., Bam, W., Estapa, M., Kenyon, J. A., et al. (2024). Carbon and silica fluxes during a declining North Atlantic spring bloom as part of the EXPORTS program. *Marine Chemistry*, *258*, 104346. https://doi.org/10.1016/j.marchem.2023.104346

Corral, Á., & González, Á. (2019). Power law size distributions in geoscience revisited. *Earth and Space Science*, *6*(5), 673–697. https://doi.org/10.1029/2018ea000479

Dall'Olmo, G., Westberry, T. K., Behrenfeld, M. J., Boss, E., & Slade, W. H. (2009). Significant contribution of large particles to optical backscattering in the open ocean. *Biogeosciences*, *6*(6), 947–967. https://doi.org/10.5194/bg-6-947-2009

Ducklow, H. W., & Carlson, C. A. (1992). Oceanic bacterial production. In K. C. Marshall (Ed.), *Advances in microbial ecology* (pp. 113–181). Springer US. https://doi.org/10.1007/978-1-4684-7609-5_3

Einstein, A. (1905). Investigations on the theory of Brownian movement. *Annalen der Physik*, *322*(8), 549–560. https://doi.org/10.1088/0031-9112/7/10/012

EXPORTS. (2018). SeaBASS [Dataset]. *NASA Ocean Biology Distributed Active Archive Center*. https://doi.org/10.5067/SEABASS/EXPORTS/DATA001

Filella, M. (2006). Colloidal properties of submicron particles in natural waters. In K. J. Wilkinson & J. R. Lead (Eds.), *Environmental colloids and particles* (Vol. 10, pp. 17–93). John Wiley & Sons, Ltd. https://doi.org/10.1002/9780470024539.ch2

Gallego-Urrea, J. A., Tuoriniemi, J., Pallander, T., & Hassellöv, M. (2010). Measurements of nanoparticle number concentrations and size distributions in contrasting aquatic environments using nanoparticle tracking analysis. *Environmental Chemistry*, *7*(1), 67–81. https://doi.org/10.1071/EN09114

Guo, L., & Santschi, P. H. (1997). Composition and cycling of colloids in marine environments. *Reviews of Geophysics*, *35*(1), 17–40. https://doi.org/10.1029/96RG03195

Jackson, G. A. (1988). Implications of high dissolved organic matter concentrations for oceanic properties and processes. *Oceanography*, *1*(2), 28–33. https://doi.org/10.5670/oceanog.1988.05

Johnson, L., Siegel, D. A., Thompson, A. F., Fields, E., Erickson, Z., Cetinic, I., et al. (2023). Assessment of oceanographic conditions during the North Atlantic EXport Processes in the Ocean from RemoTe Sensing (EXPORTS) Field Campaign. *Progress in Oceanography*, *220*, 103170. https://doi.org/10.1016/j.pocean.2023.103170

Johnson, P. W., & Sieburth, J. M. (1979). Chroococcoid cyanobacteria in the sea: A ubiquitous and diverse phototrophic biomass. *Limnology & Oceanography*, *24*(5), 928–935. https://doi.org/10.4319/lo.1979.24.5.0928

Junge, C. E. (1969). Comments on "concentration and size distribution measurements of atmospheric aerosols and a test of the theory of self-preserving size distributions". *Journal of the Atmospheric Sciences*, *26*(3), 603–608. https://doi.org/10.1175/1520-0469(1969)026<0603:coasdm>2.0.co;2

Kepkay, P. E. (1994). Particle aggregation and the biological reactivity of colloids. *Marine Ecology Progress Series*, *109*, 293–304. https://doi.org/10.3354/meps109293

Koike, I., Hara, S., Terauchi, K., & Kogure, K. (1990). Role of sub-micrometre particles in the ocean. *Nature*, *345*(6272), 242–244. https://doi.org/10.1038/345242a0

Langevin, P. (1908). On the theory of Brownian motion. *Comptes Rendus Hebdomadaires des Seances de l`Aeademie des Sciences*, *146*, 530–533. https://doi.org/10.1119/1.18725

Leipper, D. F. (1954). *Summary of North Pacific weather station bathythermograph data, 1943-1952* (7). Department of Oceanography, The Agricultural and Mechanical College of Texas, College Station. https://doi.org/10.5962/bhl.title.39214

Li, C., Chiang, K.-P., Laws, E. A., Liu, X., Chen, J., Huang, Y., et al. (2022). Quasi-antiphase diel patterns of abundance and cell size/biomass of picophytoplankton in the oligotrophic ocean. *Geophysical Research Letters*, *49*(5), e2022GL097753. https://doi.org/10.1029/2022GL097753

Loisel, H., Nicolas, J.-M., Sciandra, A., Stramski, D., & Poteau, A. (2006). Spectral dependency of optical backscattering by marine particles from satellite remote sensing of the global ocean. *Journal of Geophysical Research*, *111*(C9), C09024. https://doi.org/10.1029/2005JC003367

Longhurst, A. R., Koike, I., Li, W. K. W., Rodriguez, J., Dickie, P., Kepay, P., et al. (1992). Sub-micron particles in northwest Atlantic shelf water. *Deep-Sea Research, Part A: Oceanographic Research Papers*, *39*(1), 1–7. https://doi.org/10.1016/0198-0149(92)90016-M

McCave, I. N. (1984). Size spectra and aggregation of suspended particles in the deep ocean. *Deep-Sea Research, Part A: Oceanographic Research Papers*, *31*(4), 329–352. https://doi.org/10.1016/0198-0149(84)90088-8

Omand, M. M., D'Asaro, E. A., Lee, C. M., Perry, M. J., Briggs, N., Cetinić, I., & Mahadevan, A. (2015). Eddy-driven subduction exports particulate organic carbon from the spring bloom. *Science*, *348*(6231), 222–225. https://doi.org/10.1126/science.1260062

Organelli, E., & Dall'Olmo, G. (2018). Particle size distributions in the upper 500 m of the Atlantic Ocean from the Atlantic Meridional Transect cruise AMT26 (JR16001) using a Coulter counter [Dataset]. *British Oceanographic Data Centre, Natural Environment Research Council*. https://doi.org/10.5285/79103bda-8913-39f3-e053-6c86abc0567a

Organelli, E., Dall'Olmo, G., Brewin, R. J. W., Nencioli, F., & Tarran, G. A. (2020). Drivers of spectral optical scattering by particles in the upper 500 m of the Atlantic Ocean. *Optics Express*, *28*(23), 34147–34166. https://doi.org/10.1364/OE.408439

Reynolds, R. A., & Stramski, D. (2021). Variability in oceanic particle size distributions and estimation of size class contributions using a non-parametric approach. *Journal of Geophysical Research: Oceans*, *126*(12), e2021JC017946. https://doi.org/10.1029/2021JC017946

Ribalet, F., Berthiaume, C., Hynes, A., Jarred, S., Carlson, M., Clayton, S., et al. (2020). SeaFlow data v1: High-resolution abundance, size and biomass of small phytoplankton in the North Pacific (1.3) [Dataset]. *Zenodo*. https://doi.org/10.5281/zenodo.3994953

Richardson, T. L., & Jackson, G. A. (2007). Small phytoplankton and carbon export from the surface ocean. *Science*, *315*(5813), 838–840. https://doi.org/10.1126/science.1133471

Runyan, H., Reynolds, R. A., & Stramski, D. (2020). Evaluation of particle size distribution metrics to estimate the relative contributions of different size fractions based on measurements in Arctic waters. *Journal of Geophysical Research: Oceans*, *125*(6), e2020JC016218. https://doi.org/10.1029/2020JC016218

Sharp, J. H. (1973). Size classes of organic carbon in seawater. *Limnology & Oceanography*, *18*(44), l–447. https://doi.org/10.4319/lo.1973.18.3.0441

Sheldon, R. W., Prakash, A., & Sutcliffe, W. H. (1972). The size distribution of particles in the ocean. *Limnology & Oceanography*, *17*(3), 327–340. https://doi.org/10.4319/lo.1972.17.3.0327

Siegel, D. A., Cetinić, I., Graff, J. R., Lee, C. M., Nelson, N., Perry, M. J., et al. (2021). An operational overview of the EXport Processes in the Ocean from RemoTe Sensing (EXPORTS) Northeast Pacific field deployment. *Elementa: Science of the Anthropocene*, *9*(1), 00107. https://doi.org/10.1525/elementa.2020.00107

Stephens, B. M., Opalk, K., Petras, D., Liu, S., Comstock, J., Aluwihare, L. I., et al. (2020). Organic matter composition at Ocean Station Papa affects its bioavailability, bacterioplankton growth efficiency and the responding taxa. *Frontiers in Marine Science*, *7*(1077). https://doi.org/10.3389/fmars.2020.590273

Stramski, D., & Kiefer, D. A. (1991). Light scattering by microorganisms in the open ocean. *Progress in Oceanography*, *28*(4), 343–383. https://doi.org/10.1016/0079-6611(91)90032-H

Stramski, D., Tatarkiewicz, J. J., Reynolds, R. A., & Karr, M. (2017). Nanoparticle analyzer. United States Patent No. US 9,645,070 B2. U. S. P. T. Office.

Stramski, D., & Wozniak, S. B. (2005). On the role of colloidal particles in light scattering in the ocean. *Limnology & Oceanography*, *50*(5), 1581–1591. https://doi.org/10.4319/lo.2005.50.5.1581

Toggweiler, J. R. (1990). Diving into the organic soup. *Nature*, *345*(6272), 203–204. https://doi.org/10.1038/345203a0

Vaulot, D., & Marie, D. (1999). Diel variability of photosynthetic picoplankton in the equatorial Pacific. *Journal of Geophysical Research*, *104*(C2), 3297–3310. https://doi.org/10.1029/98JC01333

Wells, M. L., & Goldberg, E. D. (1991). Occurrence of small colloids in sea water. *Nature*, *353*(6342), 342–344. https://doi.org/10.1038/353342a0

Wells, M. L., & Goldberg, E. D. (1992). Marine submicron particles. *Marine Chemistry*, *40*(1), 5–18. https://doi.org/10.1016/0304-4203(92)90045-C

Wells, M. L., & Goldberg, E. D. (1994). The distribution of colloids in the North Atlantic and Southern Oceans. *Limnology & Oceanography*, *39*(2), 286–302. https://doi.org/10.4319/lo.1994.39.2.0286

Xiong, Y., Zhang, X., & Hu, L. (2022). A method for tracking the Brownian motion to estimate the size distribution of submicron particles in seawater. *Limnology and Oceanography: Methods*, *20*(2022), 373–386. https://doi.org/10.1002/lom3.10494

Yamasaki, A., Fukuda, H., Fukuda, R., Miyajima, T., Nagata, T., Ogawa, H., & Koike, I. (1998). Submicrometer particles in northwest Pacific coastal environments: Abundance, size distribution, and biological origins. *Limnology & Oceanography*, *43*(3), 536–542. https://doi.org/10.4319/lo.1998.43.3.0536

Zhang, X., Hu, L., Xiong, Y., Huot, Y., & Gray, D. (2020). Experimental estimates of optical backscattering associated with submicron particles in clear oceanic waters. *Geophysical Research Letters*, *47*(4), e2020GL087100. https://doi.org/10.1029/2020gl087100